Tissue Engineering

Tissue Engineering Manuscript Central: http://mc.manuscriptcentral.com/ten

3D Bioprinting of PCL Reinforced Gene Activated Bioinks for Musculoskeletal Tissue Engineering

Journal:	*Tissue Engineering*
Manuscript ID	Draft
Manuscript Type:	Invited Submission
Date Submitted by the Author:	n/a
Complete List of Authors:	Cunniffe, Grainne; Trinity College Dublin, Trinity Centre for Bioengineering, Trinity Biomedical Sciences Institute; University of Dublin Trinity College, Department of Mechanical and Manufacturing Engineering; University of Dublin Trinity College, Advanced Materials and Bioengineering Research Centre Gonzalez-Fernandez, Tomas; Trinity College Dublin, Trinity Centre for Bioengineering; University of Dublin Trinity College, Department of Mechanical and Manufacturing Engineering; University of Dublin Trinity College, Advanced Materials and Bioengineering Research Centre Daly, Andrew; Trinity College Dublin, Trinity Centre for Bioengineering, Trinity Biomedical Sciences Institute; University of Dublin Trinity College, Department of Mechanical and Manufacturing Engineering; University of Dublin Trinity College, Advanced Materials and Bioengineering Research Centre Sathy, Binulal; Trinity College Dublin, Trinity Centre for Bioengineering, Trinity Biomedical Sciences Institute; University of Dublin Trinity College, Department of Mechanical and Manufacturing Engineering; Trinity College Dublin, Advanced Materials and Bioengineering Research Centre Jeon, Oju; Case Western Reserve University, Department of Biomedical Engineering Alsberg, Eben; Case Western Reserve University, Department of Biomedical Engineering; Case Western Reserve University, Department of Orthopaedic Surgery; Case Western Reserve University, National Centre for Regenerative Medicine Kelly, Daniel; Trinity College Dublin, Trinity Centre for Bioengineering, Trinity Biomedical Sciences Institute; University of Dublin Trinity College, Department of Mechanical and Manufacturing Engineering; Trinity College Dublin, Advanced Materials and Bioengineering Research Centre
Keyword:	Bioprinting < Enabling Technologies in Tissue Engineering (DO NOT select this phrase; it is a header ONLY), Gene Therapy < Enabling Technologies in Tissue Engineering (DO NOT select this phrase; it is a header ONLY), Bone < Applications in Tissue Engineering (DO NOT select this phrase; it is a header ONLY)
Manuscript Keywords (Search Terms):	Biofabrication, Gene Activated Scaffold, Bioink, Osteogenesis, Transfection
Abstract:	Regeneration of complex bone defects remains a significant clinical

	challenge. Recently, multi-tool biofabrication has permitted the combination of various biomaterials to create multifaceted composites with tailorable mechanical properties and spatially controlled biological function. In this study we sought to use bioprinting to engineer non-viral gene activated constructs reinforced by polymeric micro-filaments. A gene activated bioink was developed using RGD-γ-irradiated alginate and nano-sized particles of hydroxyapatite (nHA) complexed to plasmid DNA (pDNA). This ink was combined with bone marrow derived mesenchymal stem cells (MSCs) and then co-printed with a polycaprolactone (PCL) supporting mesh to provide mechanical stability to the construct. Reporter genes were first used to demonstrate successful cell transfection using this system, with sustained expression of the transgene detected over14 days post bioprinting. Delivery of a combination of therapeutic genes encoding for BMP2 and TGF-β3 promoted robust osteogenesis of encapsulated MSCs in vitro, with enhanced levels of matrix deposition and mineralisation observed following the incorporation of therapeutic pDNA. Gene activated MSC-laden constructs were then implanted subcutaneously, directly post fabrication, and were found to support superior levels of vascularisation and mineralisation compared to cell-free controls. These results validate the use of a gene activated bioink to impart biological functionality to 3D bioprinted constructs.

3D Bioprinting of PCL Reinforced Gene Activated Bioinks for Musculoskeletal Tissue Engineering

Gráinne M Cunniffe [1,2,3]†, Tomas Gonzalez-Fernandez [1,2,3]†, Andrew Daly [1,2,3], Binulal N Sathy [1,2,3], Oju Jeon[4], Eben Alsberg[4,5,6], Daniel J Kelly [1,2,3*]

[1]Trinity Centre for Bioengineering, Trinity Biomedical Sciences Institute, Trinity College Dublin. [2]Department of Mechanical and Manufacturing Engineering, School of Engineering, Trinity College Dublin. [3]Advanced Materials and Bioengineering Research Centre, Trinity College Dublin and Royal College of Surgeons in Ireland. [4] Department of Biomedical Engineering, Case Western Reserve University, Cleveland, USA. [5] Department of Orthopaedic Surgery, Case Western Reserve University, Cleveland, USA. [6] National Centre for Regenerative Medicine, Case Western Reserve University, Cleveland, USA.

† Dr. Gráinne M. Cunniffe and Mr. Tomas Gonzalez-Fernandez contributed equally to this work.

*Corresponding Author

Prof. Daniel J Kelly, Trinity Centre for Bioengineering, Trinity College Dublin

Email: kellyd9@tcd.ie, Tel: 353-1896-3336

Abstract

Regeneration of complex bone defects remains a significant clinical challenge. Recently, multi-tool biofabrication has permitted the combination of various biomaterials to create multifaceted composites with tailorable mechanical properties and spatially controlled biological function. In this study we sought to use bioprinting to engineer non-viral gene activated constructs reinforced by polymeric micro-filaments. A gene activated bioink was developed using RGD-γ-irradiated alginate and nano-sized particles of hydroxyapatite (nHA) complexed to plasmid DNA (pDNA). This ink was combined with bone marrow derived mesenchymal stem cells (MSCs) and then co-printed with a polycaprolactone (PCL) supporting mesh to provide mechanical stability to the construct. Reporter genes were first used to demonstrate successful cell transfection using this system, with sustained expression of the transgene detected over14 days post bioprinting. Delivery of a combination of therapeutic genes encoding for BMP2 and TGF-β3 promoted robust osteogenesis of encapsulated MSCs *in vitro*, with enhanced levels of matrix deposition and mineralisation observed following the incorporation of therapeutic pDNA. Gene activated MSC-laden constructs were then implanted subcutaneously, directly post fabrication, and were found to support superior levels of vascularisation and mineralisation compared to cell-free controls. These results validate the use of a gene activated bioink to impart biological functionality to 3D bioprinted constructs.

Keywords: Biofabrication, Gene Activated Scaffold, Bioink, Osteogenesis, Transfection

1. Introduction

Tissue engineering and regenerative medicine approaches can be augmented through the strategic use of gene therapy (1). Non-viral gene delivery can facilitate endogenous expression of desired therapeutic proteins, which can provide a stimulus to cells, resulting in enhanced levels of matrix production and tissue formation (2, 3). Nano hydroxyapatite (nHA) based cell transfection has been shown to be a safe and easy technique capable of yielding robust osteogenesis following

administration of plasmid DNA (pDNA) encoding for relevant proteins such as bone morphogenic protein (BMP2) and transforming growth factor (TGF-β3) (4-7). Despite a relatively low transfection efficiency, nHA-pDNA complexes have been shown to be proficient at inducing a sustained expression of target proteins, both in 2D culture and when incorporated into 3D constructs to form gene activated matrices (8-10). However, to address the need for regenerating larger and challenging anatomical defects, emerging methods such as 3D bioprinting may be required to generate suitably complex solutions (11-13). An effective gene activated bioink could be integrated into such a biofabrication approach to provide biological functionality to a composite construct.

The degree of customised control offered by 3D bioprinting has enabled the production of scaled up, mechanically reinforced materials for musculoskeletal tissue engineering (14, 15). Another attractive feature of this spatial control is the ability to deposit specific biological cues in relevant locations, to drive complex tissue formation (16). An efficient gene activated bioink would be particularly beneficial in this regard as successful cell transfection could produce localised, sustained protein expression; something that is not as easily achieved through the use of growth factors as they can diffuse easily and cause non-localised effects (17). Calcium phosphate has been successfully used as a delivery vector within a 3D bioprinted alginate hydrogel previously, leading to elevated BMP-2 expression and ALP production *in vitro* (18, 19). However, no bone formation was observed after six weeks following subcutaneous implantation of this approach. In addition, more demanding defects such as load bearing bone defects may require more mechanical integrity than can be provided by a gene activated hydrogel alone (20). Hydrogels have previously been combined with various polymeric support structures in order to fabricate composite materials with both biological and mechanical functionality (21, 22). These constructs are typically cell-laden and cultured *in vitro* to engineer a mature tissue which can promote bone repair following implantation (23, 24). The inclusion of a gene activated bioink may permit the bioprinting of a material that can be implanted directly post fabrication, inducing sustained therapeutic protein expression *in vivo* and hence accelerating regeneration.

In this work we developed a gene activated bioink by combining a printable alginate hydrogel with nHA-pDNA complexes and co-printing this ink with a reinforcing polycaprolactone (PCL) scaffold to produce a gene activated 3D construct. Bone marrow derived mesenchymal stem cells (MSCs) were combined with the bioink directly before printing. The capacity of this strategy to successfully transfect MSCs was first assessed using reporter genes, before utilizing a combination of therapeutic genes encoding for BMP2 and TGF-β3 in an attempt to induce osteogenesis of MSCs *in vitro*. The final phase of the study sought to examine if a vascularised and mineralised tissue could be generated *in vivo* by implanting such MSC-laden gene activated constructs directly post bioprinting. If successful, such an approach could be potentially be used at the point of care to develop personalised gene activated implants for treating complex bone defects.

2. Materials and Methods

2.1. Plasmid propagation

Four different plasmids were used in the current study: two plasmids encoding for the reporter genes red fluorescent protein (pRFP, also called pTomato, kind donation from Prof. Gerhart Ryffel through Addgene) and luciferase (pLUC, pGaussia luciferase; New England Biolabs, Massachusetts, USA), and another two encoding for the therapeutic genes BMP2 (kind donation from Prof. Kazihusa Bessho, Kyoto University, Japan) and TGF-β3 (InvivoGen, Ireland). Plasmid amplification was performed by transforming chemically competent E-coli bacterial cells (One Shot TOP10; Biosciences, Ireland) according to the manufacturer's protocol. The transformed bacteria were cultured on LB plates with 100 mg/L ampicillin (Sigma-Aldrich, Ireland) as the selective antibiotic for the four plasmids. Bacterial colonies were harvested and inoculated in LB broth (Sigma-Aldrich, Ireland) and incubated overnight for further amplification. The harvested bacterial cells were then lysed, and the respective pDNA samples were purified using Qiagen plasmid kit (MaxiPrep Kit; Qiagen, Ireland). Nucleic acid concentration (ng/µl) was determined by analyzing the 260:280 ratio

and 230 nm measurement using NanoDrop spectrophotometer (Labtech International, Uckfield, UK). Plasmids in this study were used at a concentration of 0.5 µg plasmid per 1 µl Tris–EDTA (TE) buffer.

2.2. Preparation of nano hydroxyapatite (nHA)-pDNA complexes

The synthesis of the nano hydroxyapatite (nHA) particles was performed as previously described (25). Briefly, a solution of 12 mM sodium phosphate (Sigma-Aldrich, Ireland), containing 0.017% DARVAN 821A (RTVanderbilt, Norwalk, USA) was added to an equal volume of a 20 mM chloride solution (Sigma-Aldrich, Ireland) and filtered through a 0.2 mm filter (8). nHA-pDNA complexes were prepared by adding 37 µl of the nHA solution to 5 µg of each pDNA pre-treated with 6 µl 250 mM $CaCl_2$ (Sigma-Aldrich, Ireland).

2.3. Gene activated bioink

Low molecular weight sodium alginate (γ alginate, 58 000 g mol−1) was prepared by irradiating sodium alginate (MVG, 259 000 g mol−1, Pronova Biopolymers, Oslo, Norway) at a gamma dose of 5 Mrad, as previously described (26). RGD-modified alginates were prepared by coupling the GGGGRGDSP to the alginate using standard carbodiimide chemistry. Briefly, 10 g alginate was dissolved at 1% (w/v) in MES Buffer (0.1 m MES, 0.3 m NaCl, and pH 6.5). 274 mg sulfo-NHS (Pierce, Rockford, IL), 484 mg EDC (Sigma), and 100 mg GGGGRGDSP peptide (AIBioTech, Richmond, VA) were then added into alginate solution. The reaction was stopped and the solution was purified and lyophilised as previously described (27).

Bone marrow derived MSCs were isolated from the femoral shaft of 4 month old pigs and expanded to passage 2 in standard culture media (high glucose Dulbecco's modified eagle's medium GlutaMAX (hgDMEM), 10% (v/v) foetal bovine serum (FBS), 100 U mL^{-1} penicillin per 100 µg mL^{-1} streptomycin) prior to transfection. The nHA-pDNA complexes were prepared immediately before transfection, suspended in 500 µl of standard media and added to the MSCs. After 1 h of incubation, alginate was

added to the cells and nHA-pDNA complexes to a final concentration of 10 million cells/ml 1% alginate. Then the solution was mixed until a homogenous mixture was obtained (10).

2.4. Bioprinting gene activated constructs

Gene activated polymer/bioink scaffolds were fabricated using the 3D Discovery multi-head bioprinting system (Regen HU, Switzerland). The 3D Discovery was set up to allow for co-printing of a pneumatic driven syringes containing the bioinks alongside a fused deposition modeler (FDM) allowing for deposition of molten polycaprolactone (PCL, Sigma, Mn 45 000). First the RGD-γ alginate bioink was dissolved at 3.5 wt% and mixed thoroughly using a luer lock system with the MSCs in either nHA solution (nHA alone control) or the nHA-pDNA complexes (both containing 50 mM $CaCl_2$) to yield a gene activated bioink with 1% final alginate concentration [41]. To ensure homogeneity the suspension was mixed between syringes 25 times. The gene activated bioink solution was loaded into the pressure driven piston system and co-printed alongside PCL melted at 60° (Figure 1). A pressure of 0.2 MPa and a 25 Gauge needle were used to deposit the bioink strands. Following this, the constructs were immersed in a 100 mM $CaCl_2$ solution for 15 min to fully crosslink the bioink. The 3D Discovery was operated within a laminar flow hood to ensure sterility throughout the biofabrication process.

Constructs of dimensions 10 x 2 mm were printed for *in vitro* evaluation, while constructs 6 x 3 mm were printed for subsequent *in vivo* implantation. *In vitro* analysis was conducted over 28 days in either control medium (high glucose Dulbecco's modified eagle's medium GlutaMAX (hgDMEM), 10% (v/v) foetal bovine serum (FBS), 100 U mL^{-1} penicillin per 100 µg mL^{-1} streptomycin) or osteogenic culture conditions (high glucose Dulbecco's modified eagle's medium GlutaMAX (hgDMEM), 100 nM dexamethasone, 10 mM β-glycerol phosphate, and 0.05 mM ascorbic acid (all from Sigma-Aldrich, Ireland)) at 20% oxygen.

2.5. Live/Dead confocal microscopy

Cell viability was assessed 24 h after bioprinting using a LIVE/DEAD viability/cytotoxicity assay kit (Invitrogen, Bio-science, Ireland). Briefly, constructs were cut in half, washed in PBS followed by incubation in PBS containing 2 µM calcein AM (green fluorescence of membrane for live cells) and 4 µM ethidium homodimer-1 (red fluorescence of DNA for dead cells). Sections were again washed in PBS, imaged at magnification ×10 with an Olympus FV-1000 Point-Scanning Confocal Microscope (Southend-on-Sea, UK) at 515 and 615 nm channels and analysed using FV10-ASW 2.0 Viewer software. Live/dead semi-quantification was carried out using image J and counting n≥4 regions per sample.

2.6. Biochemical analysis

To perform biochemical analysis, constructs were digested with papain (125 mg/mL, pH 6.5) in 0.1 M sodium acetate, 5 nM L-cysteine HCl, and 0.05 M EDTA (all Sigma-Aldrich, Ireland) at 60 °C under constant rotation for 18 h. Calcium content was determined using a Sentinel Calcium Kit (Alpha Laboratories Ltd, UK) after digestion in 1 M HCl at 110 °C for 48 h. Proteoglycan content was estimated by quantifying the amount of sulfated glycosaminoglycan (sGAG) in the pellets using the dimethylmethylene blue (DMMB) dye-binding assay (Blyscan, Biocolor Ltd. Northern Ireland), with a chondroitin sulfate standard. Total collagen content was determined by measuring the hydroxyproline content. Samples were hydrolyzed at 110 °C for 18 h in concentrated HCl 38%, allowed to dry, and analyzed using a chloramine-T assay with a hydroxyproline-to-collagen ratio of 1:7.69 (28). Four samples per group were analyzed for each biochemical assay.

2.7. Reporter gene detection

RFP expression was detected using Leica SP8 scanning confocal microscope (Leica Microsystems, Ireland) 24 hours post bioprinting. Luciferase expression was imaged using a real time bioluminescence imaging system (PhotonImager, Biospace lab, France) to visualise the spatial distribution of luminescence over time. Luciferase expression in the culture media was also

quantified using a Pierce Gaussia Luciferase Flash Assay Kit (ThermoFisher, Ireland) at different time points up to 14 days.

2.8. Micro-computed tomography

Micro-computed tomography (µCT) scans were performed using a Scanco Medical 40 µCT system (Scanco Medical, Bassersdorf, Switzerland) with a 70 kVp X-ray source at 114 µA. Six constructs were analysed per *in vivo* experimental group and quantification was performed by setting a threshold of 210 corresponding to a density of 432.58 mg hydroxyapatite/cm^3) and recording the mineral volume (mm^3). N=3 samples were scanned and analysed at a threshold of 100, corresponding to 120.81 mg hydroxyapatite/cm^3 for the *in vitro* study. Reconstructed 3D images were generated from the scans and used to visualise mineral distribution throughout the constructs.

2.9. Subcutaneous Implantation

Gene activated constructs (n=9) were implanted subcutaneously into the back of nude mice (Balb/c; Harlan, UK) as previously described with three samples inserted in each of two pockets (29). The constructs were harvested after 4 and 12 weeks. Mice were euthanised by CO_2 inhalation and the animal protocol was reviewed and approved by the ethics committee of Trinity College Dublin and the Health Products Regulatory Authority (HPRA).

2.10. Statistical analysis

Statistical analysis was carried out using GraphPad software. The results are reported as means ± standard deviation and groups were analysed using Student's two-tailed t-tests or by a general linear model for analysis of variance with groups of factors. Tukey's post-hoc test was used to compare conditions. Significance was accepted at a level of $p < 0.05$.

3. Results

3.1 Gene activated bioinks support sustained expression of reporter genes following co-printing with PCL filaments

To establish that the gene activated bioink would remain functional following 3D bioprinting with a PCL support structure, reporter genes (pLUC and pRFP) were utilised to validate successful transfection of MSCs encapsulated within the bioinks at the time of bioprinting. The viability of MSCs printed within the gene activated bioink was not affected by the presence of the pDNA encoding for luciferase, however, some cell death was observed due to co-printing the cell-laden bioink with PCL (nHA-alone 64 ± 10%, nHA-pLUC 69 ± 2%, Figure 2, Supplemental Figure 1). By 14 days, the DNA content remained at the same level as that quantified at day 1 and almost 100% of cells within the construct were observed to be viable using live/dead staining.

Reporter gene analysis using red fluorescent protein (RFP) and luciferase indicated that successful transfection of bioprinted MSCs was achieved within the gene activated bioink (Figure 3). RFP was observed 24 hours post bioprinting using fluorescent microscopy to provide an initial validation of successful pDNA uptake and protein expression. Luciferase was then employed to investigate temporal expression of a reporter protein. Luciferase was found to increase in expression over 14 days of culture, as assessed both by quantifying the luciferase expressed and released into the media (Figure 3b) and by imaging the protein remaining within the constructs (Figure 3c).

3.2 Therapeutic gene delivery enhanced osteogenesis of MSCs *in vitro*

Following validation of successful transfection using reporter genes, a combination of therapeutic genes encoding for BMP2 and TGF-β3 was incorporated into the bioink system. These combinations of genes were chosen as delivery of recombinant BMP-2 and TGF-β protein from MSC-laden alginate hydrogels has previously been shown to promote bone formation *in vivo* (30). Constructs were

bioprinted and cultured for 28 days in either control medium or osteogenic culture conditions. Macroscopically, evidence of matrix deposition can be observed in all groups at this time point relative to constructs at day 0 (Figure 4). Biochemical quantification indicated that significantly higher levels of DNA and deposition of glycosaminoglycan (GAG) and collagen was achieved in both culture conditions following inclusion of pDNA within the bioink. DNA quantified at day 1 and day 14 (Supplemental Figure 1) had not indicated any differential response in DNA content between the transfected and non-transfected control groups.

Upon quantification of calcium content, the matrix was found to be mineralised, indicating the onset of osteogenesis (Figure 5). Significantly higher levels of mineral deposition were observed within the pDNA containing bioinks in control medium, and this effect was greatly amplified following culture in osteogenic supplemented medium. 3D reconstructed µCT images demonstrated the homogeneity of the mineral distribution throughout the cultured constructs.

3.3 Bioprinted gene activated constructs containing MSCs promote the development of vascularised and mineralised tissues *in vivo*

Bioprinted gene activated constructs were implanted directly post fabrication, and were compared to bioprinted acellular control constructs containing pDNA-nHA complexes only after 4 and 12 weeks *in vivo* (Figure 6 a,c). Macroscopic evidence of vascular in-growth was observable at both time points, and verified using histological analysis (Supplemental Figure 2). By 12 weeks, MSC-laden constructs appeared to be more vascularised. Regions of *de novo* bone formation and immature osteoid was also detected in the MSC-laden constructs. Mineral quantification at both time points indicated that the incorporation of MSCs resulted in significantly higher levels of mineral deposition compared to the acellular control, and that the deposition increased significantly with time (Figure 6 b,d). Distribution of mineral can be observed homogeneously throughout the construct.

4. Discussion

This study describes the successful development of a gene activated bioink capable of transfecting mesenchymal stem cells post 3D bioprinting. These MSC-laden bioinks were co-deposited alongside a reinforcing PCL network to produce composite constructs suitable for bone tissue engineering applications. Reporter genes indicated that protein expression was detected after 24 hours and that protein expression could be sustained, and in fact continued to increase, over 14 days of *in vitro* culture. Transfection with therapeutic genes encoding for BMP2 and TGF-β3 promoted enhanced osteogenesis *in vitro* compared to non-transfected controls containing only the nHA vector, implying that this gene activated bioink system could induce the expression of biologically functional proteins. Implantation of these gene activated MSC-laden constructs directly post fabrication was capable of driving vascularisation and mineralisation in a subcutaneous environment. These findings support the continued development of 3D printed gene activated scaffolds as putative 'point-of-care' treatment options for a range of musculoskeletal defects.

The choice of material for the gene activated bioink was motivated by a number of factors, including the printability of the alginate hydrogel, the presence of the RGD ligand to allow cell spreading, the ability to facilitate calcium phosphate based gene delivery and established capacity to enable the osteogenic differentiation of MSCs (10, 19, 23, 31-34). Polymeric scaffolds are typically inert and may require supplementation with various factors in order to induce a favourable biological response, often provided through the addition of extracellular matrix components, or exogenous growth factors (35-38). A number of publications have also reported superior biological activity solely due to the addition of alginate hydrogel to PCL scaffolds (39, 40). Furthermore, alginate has a tunable degradation rate, tailorable mechanical properties, and already has FDA approval for other indications (27).

The temporal production of gene product observed over 14 days of culture clearly demonstrates the potential of this gene activated bioink approach for sustained therapeutic protein

delivery, especially when compared to the burst release profiles typically observed with traditional growth factor delivery hydrogels. By employing the cells themselves to express the desired protein, limitations with protein delivery including rapid degradation of potentially supra-physiological, toxic doses, and dispersion of the drug to dangerous locations can be overcome (41). The bioprinting process itself, or the fact that the bioinks were co-deposited alongside molten PCL, does not seem to detract from the ability of the non-viral delivery vector nHA to successfully transfect cells. In fact, the intensity of luciferase signal increased over 14 days of culture, suggesting sustained transfection of encapsulated MSCs following the bioprinting process.

Having demonstrated it was possible to bioprint gene activated constructs reinforced by a network of PCL micro-filaments, the capacity of this system to promote MSC differentiation along the osteogenic pathway was then tested. Alginate is commonly used as a biomaterial in bone regeneration strategies (19, 26, 31, 42, 43), and more recently has been used as a bioink for bone and cartilage bioprinting (18, 34, 41, 44). In the absence of osteogenic supplements, the co-delivery of BMP-2 and TGFβ3 pDNA within these MSC-laden alginate bioinks resulted in the deposition of a mineralised matrix, with the differences compared to non-transfected controls becoming particularly apparent when cultured in osteogenic conditions. The nHA particles used to deliver the plasmids may be providing an osteogenic stimulus, although the concentration used to deliver pDNA is relatively low compared to that used previously to induce mineralisation (45-47). Furthermore, it has previously been shown that while nHA transfects cells with lower efficacies to other vectors, its use still promotes higher overall levels of osteogenesis (45). In a previous study we observed that nHA-mediated delivery of TGF-β3 and BMP2 in an alginate hydrogel promoted a more chondrogenic rather than osteogenic stimulus (10). This may be explained by the conditions (normoxia and osteogenic media) and the RGD modification of the alginate which we implemented in this study to promote direct osteogenic differentiation of encapsulated MSCs. Together these findings support the use of alginate hydrogels containing pDNA-nHA complexes as gene activated bioinks for bone tissue engineering.

Bioprinted gene activated constructs became well vascularised *in vivo*, supporting the development of a mineralised bone-like tissue. These *in vivo* results point to the benefit of including mesenchymal stem cells when developing 'point-of-care' bioprinted constructs for bone regeneration. Mineralisation was considerably higher at both 4 and 12 weeks in the MSC-laden constructs compared to the acellular control. It could be argued however, that the acellular, pDNA containing group may perform better upon implantation into an orthotopic defect site compared to the subcutaneous site due to the likelihood of greater infiltration of host osteo-progenitor cells. A study investigating the use of pDNA encoding for BMP2 and delivered using an alginate hydrogel based non-viral approach also reported enhanced results when the gene activated biomaterial was combined with MSCs (44). Histological evidence of blood vessels in-growth was detected in both acellular and MSC-laden constructs by 12 weeks, and mineralisation was observed to increase with time *in vivo* corresponding with evidence of *de novo* immature bone formation at this later time point. This result agrees with previous *in vivo* studies delivering a combination of BMP2 and TGF-β3, either as recombinant proteins or through the use of gene delivery (30, 48).

5. Conclusion

The treatment of challenging fractures and large osseous defects presents a formidable clinical problem. Recently, multi-tool biofabrication has permitted combination of various materials to create complex composite implants with tailorable mechanical properties and spatially controlled biological function. This study validated the efficiency of a gene activated bioink to induce cell transfection within a 3D bioprinted PCL-bioink composite construct. Sustained protein expression was achieved for up to 14 days post bioprinting, and the combined delivery of the therapeutic genes BMP2 and TGF-β3 led to enhanced osteogenesis of MSCs *in vitro* and formation of a vascularised and mineralised tissue upon subcutaneous implantation. These results demonstrate an effective

platform technology to enrich biofabrication techniques with gene activated bioinks for musculoskeletal applications.

6. References

1. Evans C. Using genes to facilitate the endogenous repair and regeneration of orthopaedic tissues. Int Orthop **38,** 1761, 2014.
2. Li S-D, Huang L. Non-viral is superior to viral gene delivery. J Control Release **123,** 181, 2007.
3. Santos J, L. , Pandita D, Rodrigues J, Pego A, P., Granja P, L. , Tomas H. Non-Viral Gene Delivery to Mesenchymal Stem Cells: Methods, Strategies and Application in Bone Tissue Engineering and Regeneration. Curr Gene Ther **11,** 46, 2011.
4. Olton D, Li J, Wilson ME, Rogers T, Close J, Huang L, et al. Nanostructured calcium phosphates (NanoCaPs) for non-viral gene delivery: influence of the synthesis parameters on transfection efficiency. Biomaterials **28,** 1267, 2007.
5. Xie Y, Chen Y, Sun M, Ping Q. A mini review of biodegradable calcium phosphate nanoparticles for gene delivery. Curr Pharm Biotechnol **14,** 918, 2013.
6. Dang PN, Dwivedi N, Phillips LM, Yu X, Herberg S, Bowerman C, et al. Controlled Dual Growth Factor Delivery From Microparticles Incorporated Within Human Bone Marrow-Derived Mesenchymal Stem Cell Aggregates for Enhanced Bone Tissue Engineering via Endochondral Ossification. Stem Cells Transl Med **5,** 206, 2016.
7. Lin Y, Tang W, Wu L, Jing W, Li X, Wu Y, et al. Bone regeneration by BMP-2 enhanced adipose stem cells loading on alginate gel. Histochem Cell Biol **129,** 203, 2008.
8. Curtin CM, Cunniffe GM, Lyons FG, Bessho K, Dickson GR, Duffy GP, et al. Innovative collagen nano-hydroxyapatite scaffolds offer a highly efficient non-viral gene delivery platform for stem cell-mediated bone formation. Adv Mater **24,** 749, 2012.
9. Choi S, Yu X, Jongpaiboonkit L, Hollister SJ, Murphy WL. Inorganic coatings for optimized non-viral transfection of stem cells. Sci Rep **3,** 1567, 2013.
10. Gonzalez-Fernandez T, Tierney EG, Cunniffe GM, O'Brien FJ, Kelly DJ. Gene Delivery of TGF-beta3 and BMP2 in an MSC-Laden Alginate Hydrogel for Articular Cartilage and Endochondral Bone Tissue Engineering. Tissue Eng Part A **22,** 776, 2016.
11. Do A-V, Khorsand B, Geary SM, Salem AK. 3D Printing of Scaffolds for Tissue Regeneration Applications. Adv Healthc Mater **4,** 1742, 2015.
12. Melchels FP, Blokzijl MM, Levato R, Peiffer QC, Ruijter M, Hennink WE, et al. Hydrogel-based reinforcement of 3D bioprinted constructs. Biofabrication **8,** 035004, 2016.
13. Murphy SV, Atala A. 3D bioprinting of tissues and organs. Nat Biotechnol **32,** 773, 2014.
14. Visser J, Melchels FPW, Jeon JE, van Bussel EM, Kimpton LS, Byrne HM, et al. Reinforcement of hydrogels using three-dimensionally printed microfibres. Nat Commun **6,** 6933, 2015.
15. Malda J, Visser J, Melchels FP, Jüngst T, Hennink WE, Dhert WJA, et al. 25th Anniversary Article: Engineering Hydrogels for Biofabrication. Adv Mater **25,** 5011, 2013.
16. Cooper GM, Miller ED, Decesare GE, Usas A, Lensie EL, Bykowski MR, et al. Inkjet-based biopatterning of bone morphogenetic protein-2 to spatially control calvarial bone formation. Tissue Eng Part A **16,** 1749, 2010.
17. Bonadio J, Smiley E, Patil P, Goldstein S. Localized, direct plasmid gene delivery in vivo: prolonged therapy results in reproducible tissue regeneration. Nat Med **5,** 753, 1999.
18. Loozen LD, Wegman F, Oner FC, Dhert WJA, Alblas J. Porous bioprinted constructs in BMP-2 non-viral gene therapy for bone tissue engineering. J Mater Chem B **1,** 6619, 2013.
19. Krebs MD, Salter E, Chen E, Sutter KA, Alsberg E. Calcium phosphate-DNA nanoparticle gene delivery from alginate hydrogels induces in vivo osteogenesis. J Biomed Mater Res A **92,** 1131, 2010.

20. Billiet T, Vandenhaute M, Schelfhout J, Van Vlierberghe S, Dubruel P. A review of trends and limitations in hydrogel-rapid prototyping for tissue engineering. Biomaterials **33,** 6020, 2012.

21. Boere KW, Visser J, Seyednejad H, Rahimian S, Gawlitta D, van Steenbergen MJ, et al. Covalent attachment of a three-dimensionally printed thermoplast to a gelatin hydrogel for mechanically enhanced cartilage constructs. Acta Biomater **10,** 2602, 2014.

22. Xu T, Binder KW, Albanna MZ, Dice D, Zhao W, Yoo JJ, et al. Hybrid printing of mechanically and biologically improved constructs for cartilage tissue engineering applications. Biofabrication **5,** 015001, 2013.

23. Daly AC, Cunniffe GM, Sathy BN, Jeon O, Alsberg E, Kelly DJ. 3D Bioprinting of Developmentally Inspired Templates for Whole Bone Organ Engineering. Adv Healthc Mater **5,** 2353, 2016.

24. Schuurman W, Levett PA, Pot MW, van Weeren PR, Dhert WJA, Hutmacher DW, et al. Gelatin-methacrylamide hydrogels as potential biomaterials for fabrication of tissue-engineered cartilage constructs. Macromol Biosci **13,** 551, 2013.

25. Cunniffe GM, O'Brien FJ, Partap S, Levingstone TJ, Stanton KT, Dickson GR. The synthesis and characterization of nanophase hydroxyapatite using a novel dispersant-aided precipitation method. J Biomed Mater Res A **95,** 1142, 2010.

26. Alsberg E, Kong HJ, Hirano Y, Smith MK, Albeiruti A, Mooney DJ. Regulating Bone Formation via Controlled Scaffold Degradation. J Dent Res **82,** 903, 2003.

27. Jeon O, Powell C, Ahmed SM, Alsberg E. Biodegradable, photocrosslinked alginate hydrogels with independently tailorable physical properties and cell adhesivity. Tissue Eng Part A **16,** 2915, 2010.

28. Ignat'eva NY, Danilov NA, Averkiev SV, Obrezkova MV, Lunin VV, Sobol EN. Determination of hydroxyproline in tissues and the evaluation of the collagen content of the tissues. J Anal Chem **62,** 51, 2007.

29. Cunniffe GM, Vinardell T, Murphy JM, Thompson EM, Matsiko A, O'Brien FJ, et al. Porous decellularized tissue engineered hypertrophic cartilage as a scaffold for large bone defect healing. Acta Biomater **23,** 82, 2015.

30. Simmons CA, Alsberg E, Hsiong S, Kim WJ, Mooney DJ. Dual growth factor delivery and controlled scaffold degradation enhance in vivo bone formation by transplanted bone marrow stromal cells. Bone **35,** 562, 2004.

31. Cunniffe GM, Vinardell T, Thompson EM, Daly AC, Matsiko A, O'Brien FJ, et al. Chondrogenically primed mesenchymal stem cell-seeded alginate hydrogels promote early bone formation in critically-sized defects. Eur Polym J **72,** 464, 2015.

32. Kundu J, Shim J-H, Jang J, Kim S-W, Cho D-W. An additive manufacturing-based PCL–alginate–chondrocyte bioprinted scaffold for cartilage tissue engineering. J Tissue Eng Regen Med **9,** 1286, 2015.

33. Venkatesan J, Bhatnagar I, Manivasagan P, Kang K-H, Kim S-K. Alginate composites for bone tissue engineering: A review. Int J Biol Macromolec **72,** 269, 2015.

34. Wegman F, Bijenhof A, Schuijff L, Oner FC, Dhert WJ, Alblas J. Osteogenic differentiation as a result of BMP-2 plasmid DNA based gene therapy in vitro and in vivo. Eur Cell Mater **21,** 230, 2011.

35. Sadr N, Pippenger BE, Scherberich A, Wendt D, Mantero S, Martin I, et al. Enhancing the biological performance of synthetic polymeric materials by decoration with engineered, decellularized extracellular matrix. Biomaterials **33,** 5085, 2012.

36. Pati F, Song TH, Rijal G, Jang J, Kim SW, Cho DW. Ornamenting 3D printed scaffolds with cell-laid extracellular matrix for bone tissue regeneration. Biomaterials **37,** 230, 2015.

37. Shim JH, Kim SE, Park JY, Kundu J, Kim SW, Kang SS, et al. Three-dimensional printing of rhBMP-2-loaded scaffolds with long-term delivery for enhanced bone regeneration in a rabbit diaphyseal defect. Tissue Eng Part A **20,** 1980, 2014.

38. Lee HJ, Kim YB, Ahn SH, Lee JS, Jang CH, Yoon H, et al. A New Approach for Fabricating Collagen/ECM-Based Bioinks Using Preosteoblasts and Human Adipose Stem Cells. Adv Healthc Mater **4,** 1359, 2015.
39. Kim YB, Kim GH. PCL/Alginate Composite Scaffolds for Hard Tissue Engineering: Fabrication, Characterization, and Cellular Activities. ACS Comb Sci **17,** 87, 2015.
40. Grandi C, Di Liddo R, Paganin P, Lora S, Dalzoppo D, Feltrin G, et al. Porous alginate/poly(epsilon-caprolactone) scaffolds: preparation, characterization and in vitro biological activity. Int J Mol Med **27,** 455, 2011.
41. Wegman F, van der Helm Y, Oner FC, Dhert WJ, Alblas J. Bone morphogenetic protein-2 plasmid DNA as a substitute for bone morphogenetic protein-2 protein in bone tissue engineering. Tissue Eng Part A **19,** 2686, 2013.
42. Augst AD, Kong HJ, Mooney DJ. Alginate Hydrogels as Biomaterials. Macromol Biosci **6,** 623, 2006.
43. Sheehy EJ, Mesallati T, Vinardell T, Kelly DJ. Engineering cartilage or endochondral bone: A comparison of different naturally derived hydrogels. Acta Biomater **13,** 245, 2015.
44. Loozen LD, van der Helm YJM, Öner FC, Dhert WJA, Kruyt MC, Alblas J. Bone Morphogenetic Protein-2 Nonviral Gene Therapy in a Goat Iliac Crest Model for Bone Formation. Tissue Eng Part A **21,** 1672, 2015.
45. Curtin CM, Tierney EG, McSorley K, Cryan SA, Duffy GP, O'Brien FJ. Combinatorial Gene Therapy Accelerates Bone Regeneration: Non-Viral Dual Delivery of VEGF and BMP2 in a Collagen-Nanohydroxyapatite Scaffold. Adv Healthc Mater **4,** 223, 2014.
46. Cunniffe GM, Dickson GR, Partap S, Stanton KT, O'Brien FJ. Development and characterisation of a collagen nano-hydroxyapatite composite scaffold for bone tissue engineering. J Mater Sci Mater Med **21,** 2293, 2010.
47. Cunniffe GM, Curtin CM, Thompson EM, Dickson GR, O'Brien FJ. Content-Dependent Osteogenic Response of Nanohydroxyapatite: An in Vitro and in Vivo Assessment within Collagen-Based Scaffolds. ACS Appl Mater Interfaces **8,** 23477, 2016.
48. Oest ME, Dupont KM, Kong HJ, Mooney DJ, Guldberg RE. Quantitative assessment of scaffold and growth factor-mediated repair of critically sized bone defects. J Orthop Res **25,** 941, 2007.

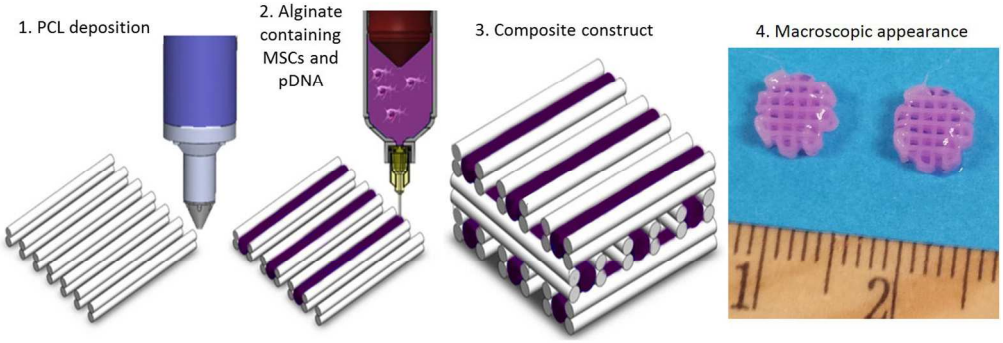

Figure 1. Schematic representation of the bioprinting process, with co-deposition of PCL and the gene activated bioink comprising of alginate, nHA-pDNA complexes and MSCs, and the macroscopic appearance of the constructs prior to implantation.

258x92mm (150 x 150 DPI)

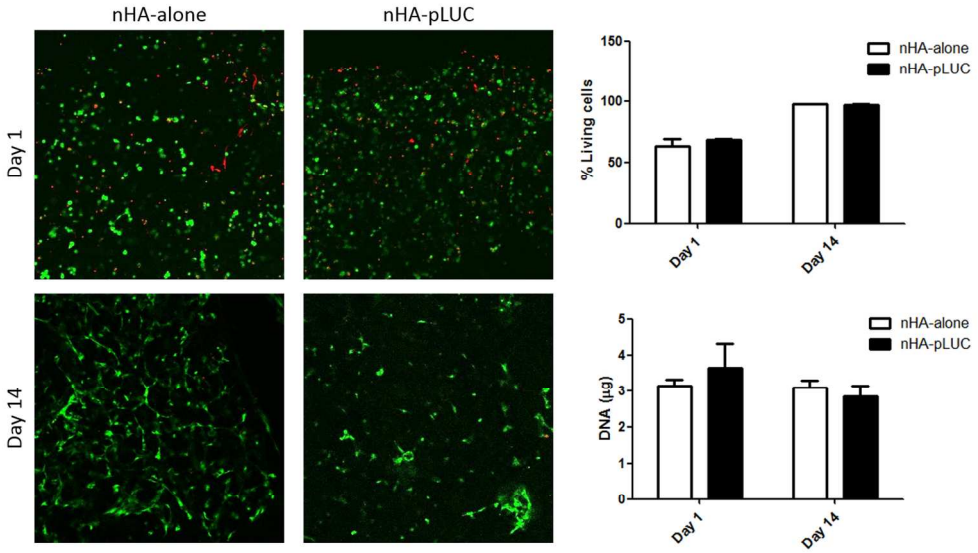

Figure 2. Cell viability is maintained following pDNA incorporation. Live/dead images demonstrate the presence of viable cells (green) at both day 1 and day 14 post bioprinting, while quantification of DNA indicated no difference between groups cultured with or without pDNA encoding for luciferase.

254x162mm (150 x 150 DPI)

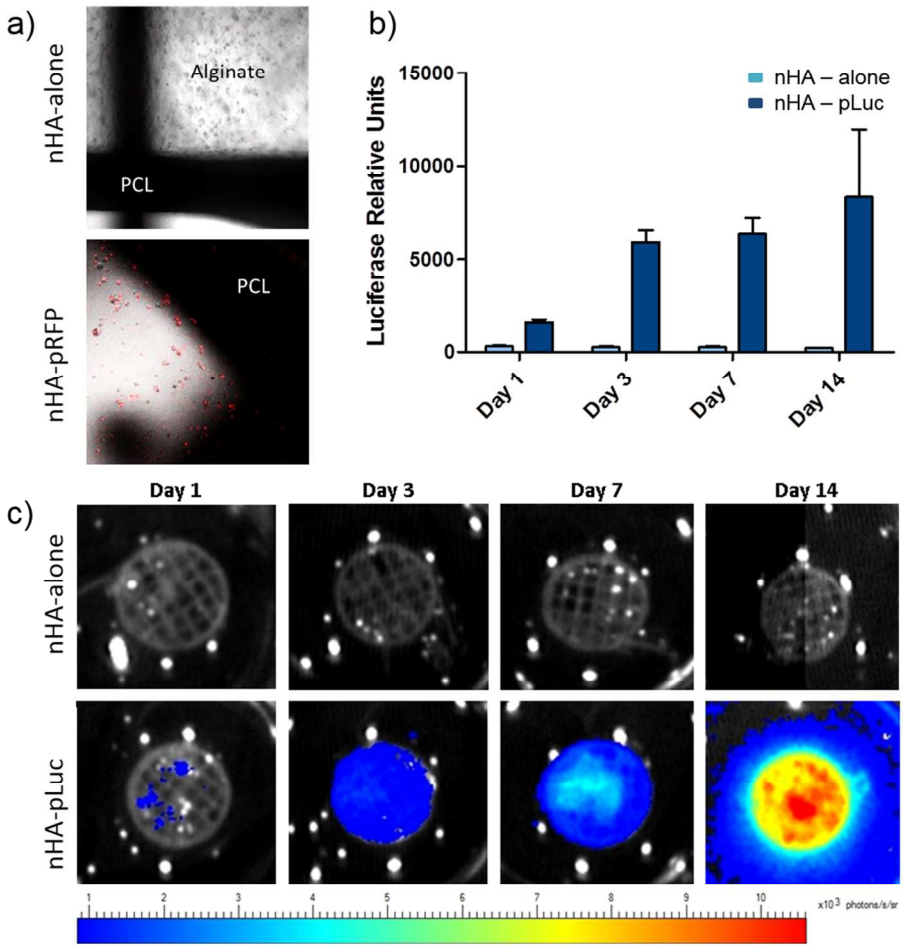

Figure 3. (a) Positive expression of red fluorescent protein (RFP) was detected 24 hours post bioprinting. (b,c) Luciferase expression was quantified and imaged for 14 days post bioprinting, demonstrating a sustained and increasing expression profile over time.

198x200mm (150 x 150 DPI)

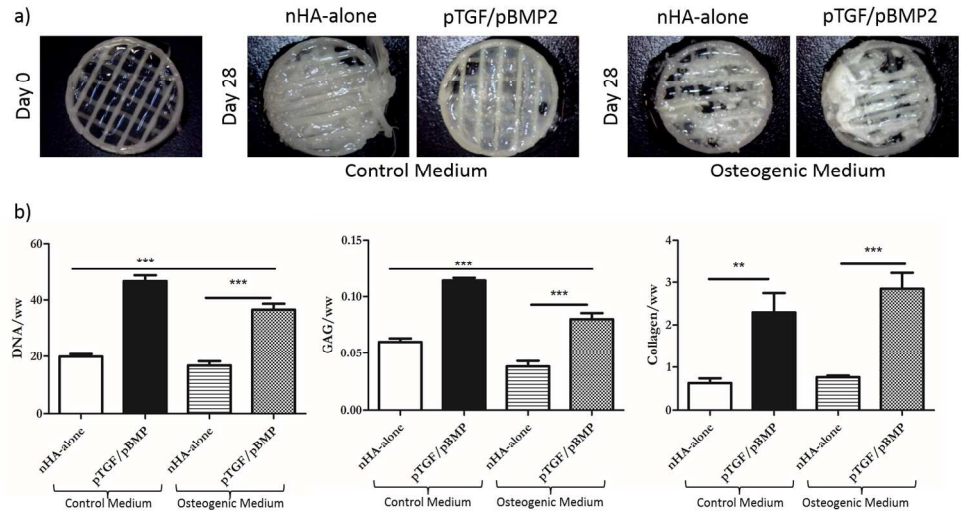

Figure 4. (a) Macroscopic appearance of bioprinted constructs immediately post bioprinting, and following 28 days in either control or osteogenic media. (b) Biochemical analysis revealed significantly higher levels of DNA in addition to glycosaminoglycan (GAG) and collagen deposition was achieved following pDNA incorporation vs. nHA-alone controls. **p<0.01, ***p<0.001

296x160mm (150 x 150 DPI)

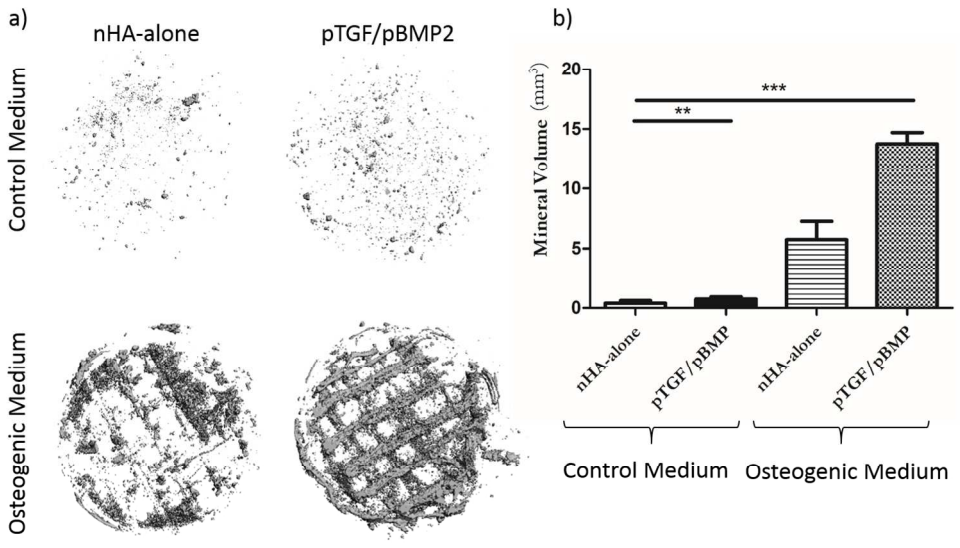

Figure 5. (a) 3D reconstructed images and (b) quantification of mineral deposition over 28 days in vitro demonstrating superior deposition was detected in the pDNA containing groups. **p<0.01, ***p<0.001

255x151mm (150 x 150 DPI)

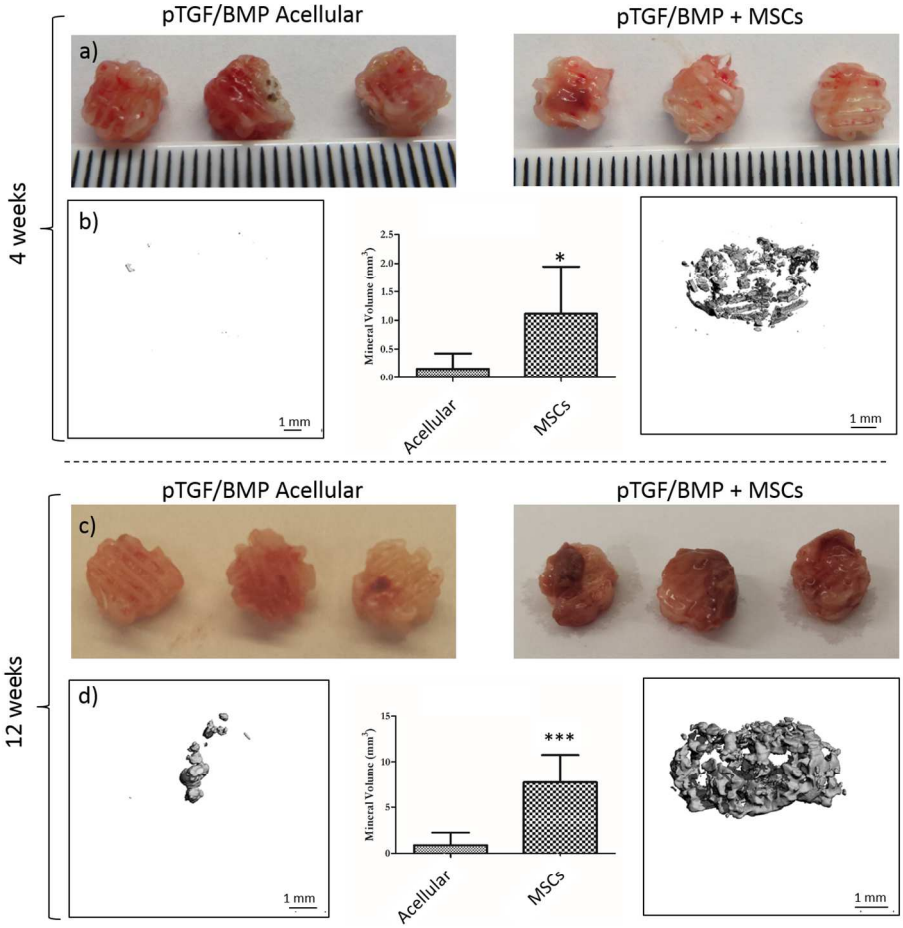

Figure 6. (a) Macroscopic appearance of acellular and MSC-laden bioprinted constructs 4 weeks post subcutaneous implantation. (b) Visualisation and quantification of mineral deposition after 4 weeks in vivo. (c, d) Macroscopic appearance and mineralisation following 12 weeks in vivo. *p<0.05, ***p<0.001

256x254mm (150 x 150 DPI)

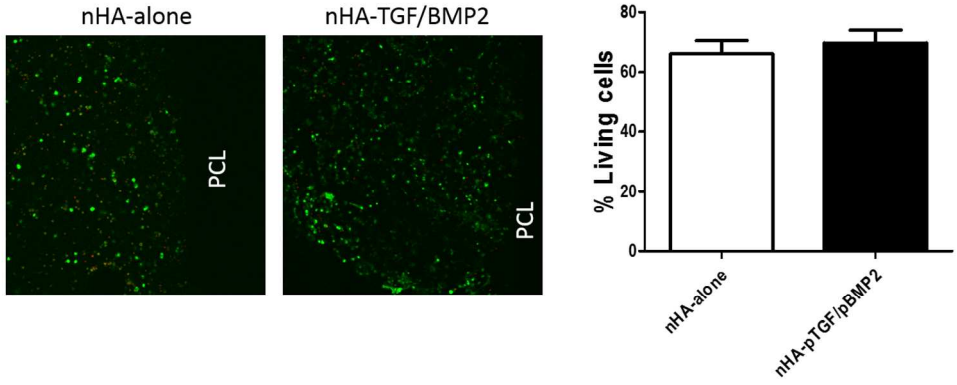

Supplemental Figure 1. Cells remain viable within 3D bioprinted constructs containing pDNA encoding for TGF-β3 and BMP2. Quantification indicated approximately 68% viable cells 24 hours post bioprinting.

244x103mm (150 x 150 DPI)

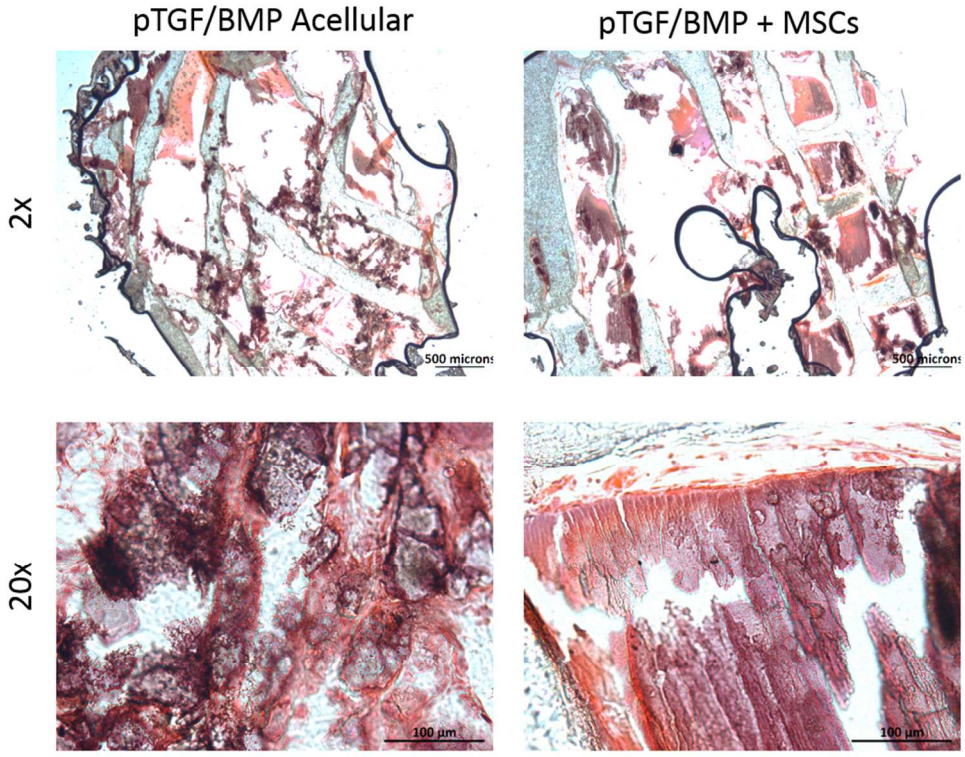

Supplemental Figure 2. Histological evaluation using Haematoxylin and Eosin staining 12 weeks post implantation indicated evidence of vascularisation and de novo bone formation in both MSC-laden and acellular constructs.

183x144mm (150 x 150 DPI)

Figure legends

Figure 1. Schematic representation of the bioprinting process, with co-deposition of PCL and the gene activated bioink comprising of alginate, nHA-pDNA complexes and MSCs, and the macroscopic appearance of the constructs prior to implantation.

Figure 2. Cell viability is maintained following pDNA incorporation. Live/dead images demonstrate the presence of viable cells (green) at both day 1 and day 14 post bioprinting, while quantification of DNA indicated no difference between groups cultured with or without pDNA encoding for luciferase.

Figure 3. (a) Positive expression of red fluorescent protein (RFP) was detected 24 hours post bioprinting. (b,c) Luciferase expression was quantified and imaged for 14 days post bioprinting, demonstrating a sustained and increasing expression profile over time.

Figure 4. (a) Macroscopic appearance of bioprinted constructs immediately post bioprinting, and following 28 days in either control or osteogenic media. (b) Biochemical analysis revealed significantly higher levels of DNA in addition to glycosaminoglycan (GAG) and collagen deposition was achieved following pDNA incorporation vs. nHA-alone controls. **p<0.01, ***p<0.001

Figure 5. (a) 3D reconstructed images and (b) quantification of mineral deposition over 28 days *in vitro* demonstrating superior deposition was detected in the pDNA containing groups. **p<0.01, ***p<0.001

Figure 6. (a) Macroscopic appearance of acellular and MSC-laden bioprinted constructs 4 weeks post subcutaneous implantation. (b) Visualisation and quantification of mineral deposition after 4 weeks *in vivo.* (c, d) Macroscopic appearance and mineralisation following 12 weeks *in vivo.* *p<0.05, ***p<0.001